J. Fluid Mech. (1990), *vol.* 212, *pp.* 533–556
Printed in Great Britain

A simple and unifying physical interpretation of scalar fluctuation measurements from many turbulent shear flows

By P. C. CHATWIN[1] AND PAUL J. SULLIVAN[2]

[1] Department of Mathematics and Statistics, Brunel University, Uxbridge, UB8 3PH, UK

[2] Department of Applied Mathematics, University of Western Ontario, London, Canada N6A 5B9

(Received 1 February 1989)

It is shown that measurements of the statistical properties of the concentration distributions of dispersing scalars taken from many different turbulent shear flows have a great number of common features. In particular the same simple relationship between the mean concentration and the mean-square fluctuation is shown to hold in all the flows, and this relationship is derived theoretically from well-known results for the unreal case when there is no molecular diffusion by a natural hypothesis about the effects of molecular diffusion. Application of the hypothesis to the higher moments and shape parameters gives results that agree reasonably well with the data (given the unavoidable experimental errors). The hypothesis should be subjected to further experimental analysis, and could simplify the application of turbulence closures and similar models. Extensions of the ideas to the probability density function of the scalar concentration suggest that it becomes self-similar. A final conclusion is that more attention to experimental errors due to instrument smoothing is highly desirable.

1. Introduction

This paper is concerned with the statistical properties of scalars dispersing in turbulent shear flows and, more particularly, with the interpretation of many sets of measurements of such properties. It seems appropriate that this paper should appear in a volume in honour of Professor George Batchelor since its aim is the same as that of his pioneering and characteristically distinctive work on homogeneous scalar fields (Batchelor 1959; Batchelor, Howells & Townsend 1959), namely to increase understanding of the effects of the basic processes of advection and molecular diffusion. This aim is common to all research on turbulent diffusion, whether experimental or theoretical, but the methodology of the present work is unusual in that it does not consider one particular flow but searches for, and identifies, features that data from a wide variety of flows have in common. These common features are consistent, broadly, with a very simple physical framework, and this fact has consequences that seem important, and are discussed.

It is useful first to summarize the basic terminology and notation that will be used throughout. Consider an ensemble of realizations of any particular dispersion experiment. Let $\Gamma(\boldsymbol{x}, t)$ denote the concentration of the scalar (in arbitrary units) at

position $\boldsymbol{x}$ and time t in one realization, and let $p(\theta;\boldsymbol{x},t)$ be the probability density function (p.d.f.) of $\Gamma(\boldsymbol{x},t)$ for the specified ensemble. Thus, for $\theta \geqslant 0$,

$$p(\theta;\boldsymbol{x},t) = \frac{\mathrm{d}}{\mathrm{d}\theta}[\mathrm{prob}\{\Gamma(\boldsymbol{x},t) \leqslant \theta\}]. \tag{1.1}$$

(Although the term concentration will be used throughout, the whole paper applies also to cases where the scalar is heat and $\Gamma(\boldsymbol{x},t)$ is the temperature difference from an ambient.) All statistical properties of Γ considered in this paper can be defined in terms of p. For example, the (ensemble) mean concentration $C(\boldsymbol{x},t)$ satisfies

$$C(\boldsymbol{x},t) = \int_0^\infty \theta p(\theta;\boldsymbol{x},t)\,\mathrm{d}\theta. \tag{1.2}$$

Of course $C(\boldsymbol{x},t)$ is the same mean concentration that occurs in the Reynolds decomposition

$$\Gamma(\boldsymbol{x},t) = C(\boldsymbol{x},t)+c(\boldsymbol{x},t); \quad \bar{\Gamma} = C, \quad \bar{c} = 0, \tag{1.3}$$

where the overbar denotes an ensemble mean, and $c(\boldsymbol{x},t)$ is the concentration fluctuation. The mean-square fluctuation $\overline{c^2}(\boldsymbol{x},t)$ is the variance of $\Gamma(\boldsymbol{x},t)$ and therefore satisfies

$$\overline{c^2}(\boldsymbol{x},t) = \int_0^\infty (\theta-C)^2 p(\theta;\boldsymbol{x},t)\,\mathrm{d}\theta = \int_0^\infty \theta^2 p(\theta;\boldsymbol{x},t)\,\mathrm{d}\theta - C^2; \tag{1.4}$$

higher moments ($\overline{c^3}(\boldsymbol{x},t), \overline{c^4}(\boldsymbol{x},t),\ldots$) are defined analogously.

In general, and this includes most applications to oceanic and atmospheric dispersion, $p(\theta;\boldsymbol{x},t)$ depends explicitly on all three components of $\boldsymbol{x}$ and on t; in such circumstances ensemble means like $C(\boldsymbol{x},t)$ and $\overline{c^2}(\boldsymbol{x},t)$ can be estimated from experiments only by appropriate arithmetical averages over a (sufficiently large) number of repeat realizations. However, in the common laboratory situation when $p(\theta;\boldsymbol{x},t)$ is independent of t, so are properties like $C, \overline{c^2},\ldots$, and they can then be estimated by time averages of the record of one realization according to the ergodic principle. All data considered in this paper belong to this latter category.

2. Some data on C and $\overline{c^2}$

Table 1 gives information about some typical experiments on scalar dispersion, but conducted in a variety of self-similar turbulent shear flows. It is clear that these also encompass several different scalar contaminants, including heat and smoke, and a range of measurement techniques.

Despite the differences in the configurations, all the experiments in table 1 (and nearly all similar ones that have been examined) have two common features.

First, in each case, the profiles of C and $\overline{c^2}$ are themselves self-similar (or approaching self-similarity). Let z denote distance downstream from the (effective) source in the direction of mean flow and let $C_0(z)$ denote the maximum value of C at each cross-section. In cases like jets and wakes, $C_0(z)$ is the centreline value and, for turbulent boundary layers with the source at the wall, it is the wall value. The self-similar structure observed in the profiles of C and $\overline{c^2}$ shows that there is a transverse lengthscale $L(z)$ which, when used to non-dimensionalize the transverse coordinate(s) in plane or cylindrical geometry, produces a dimensionless transverse coordinate η such that, for sufficiently large z,

$$C(\boldsymbol{x}) = C_0(z)F(\eta); \quad \overline{c^2}(\boldsymbol{x}) = C_0^2(z)f(\eta), \tag{2.1}$$

NO.	WORKERS	FLOW	SCALAR	MEASUREMENT TECHNIQUE
(1)	Becker *et al.* (1967)	Round jet	Oil smoke	Light-scatter
(2)	LaRue & Libby (1974)	Plane wake	Heat	Platinum wire resistance thermometer
(3)	Antonia *et al.* (1975)	Round jet with coflowing stream	Heat	Platinum/10% rhodium wire
(4)	Sreenivasan, Danh & Antonia (1976)	Smooth-walled boundary layer	Heat	Wollaston wire
(5)	Shaughnessy & Morton (1977)	Round jet exhausting into a secondary air flow	Smoke particles	Light scatter
(6)	Birch *et al.* (1978)	Round methane jet	Methane	Raman scattering of laser light
(7)	Gad-el-Hak & Morton (1979)	Grid turbulence	Smoke particles	Laser anemometer
(8)	Fackrell & Robins (1982)	Rough-walled boundary layer	Propane/ helium mixture	Flame ionisation detector system
(9)	Antonia *et al.* (1983*a*)	Plane jet	Heat	Wollaston wire

TABLE 1. Experiments in which profiles of C and $\overline{c^2}$ were measured

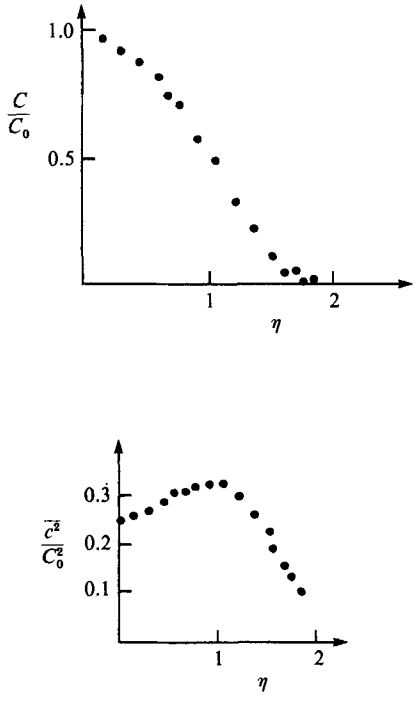

FIGURE 1. Data from Antonia *et al.* (1975).

with $F(0) = 1$ because of the definition of $C_0(z)$. In most flows, including all those in table 1, $F(\eta)$ is Gaussian, or approximately so.

The second feature that all the experiments in table 1 have in common is that $f(\eta)$ in (2.1) has a maximum at a non-zero value of η of order 1. Figure 1, adapted from Antonia, Prabhu & Stephenson (1975), is entirely typical of all the datasets.

3. A simple framework and its development

The features that have just been identified appear to be very robust; in particular the second feature occurs whatever the type of shear flow, or dispersing scalar, or measurement technique. It does not appear to matter whether the scalar is passive, or not.

Use of a simple framework helps understanding of this behaviour and aspects of it were discussed in many of the papers listed in table 1 and elsewhere (e.g. Chevray & Tutu 1977; Chatwin & Sullivan 1987*a*, *b*). Consider, for a moment, dispersion of a scalar in a turbulent shear flow in the hypothetical situation when there is no molecular diffusion (or when molecular diffusion has negligible effect). Suppose that the concentration at the source is uniform and equal to θ_1; the assumption of uniformity applies to all the experiments in table 1. Then $p(\theta; \boldsymbol{x}, t)$, the p.d.f. of concentration defined in (1.1), must have the familiar structure:

$$p(\theta; \boldsymbol{x}, t) = \pi(\boldsymbol{x}, t)\,\delta(\theta - \theta_1) + \{1 - \pi(\boldsymbol{x}, t)\}\,\delta(\theta). \tag{3.1}$$

In (3.1), $\pi(\boldsymbol{x}, t)$ is the intermittency factor, i.e. the probability that $\Gamma(\boldsymbol{x}, t) > 0$. For this hypothetical situation $\pi(\boldsymbol{x}, t)$ is also of course the probability that the fluid particle that happens to be at position $\boldsymbol{x}$ at time t emanated from the source; see Chatwin & Sullivan (1989*a*, *b*).

It now follows from (1.2) and (1.4) that

$$C(\boldsymbol{x}, t) = \theta_1 \pi; \quad \overline{c^2}(\boldsymbol{x}, t) = \theta_1^2 \pi(1 - \pi), \tag{3.2}$$

and, on eliminating π, that

$$\overline{c^2} = C(\theta_1 - C) = (\tfrac{1}{2}\theta_1)^2 - (C - \tfrac{1}{2}\theta_1)^2. \tag{3.3}$$

Hence, in this hypothetical situation, $\overline{c^2}$ has a maximum value of $\frac{1}{4}\theta_1^2$ which it takes at all points on the surface $C(\boldsymbol{x}, t) = \frac{1}{2}\theta_1$. The schematic figure 2 shows the transverse and axial variations of $\overline{c^2}/\theta_1^2$ predicted by (3.3) for a case when

$$C(\boldsymbol{x}) = C_0(z) \mathrm{e}^{-\frac{1}{2}\eta^2}, \quad \frac{C_0(z)}{\theta_1} = \frac{17.5d}{(z - 5d)}, \tag{3.4}$$

for $z \gg d$, where d is the source diameter. While (3.4) is typical of observed behaviour in jets (Becker, Hottel & Williams 1967), the main features of figure 2 are independent of (3.4); indeed (3.3) – and therefore the general properties of the curves in figure 2 – does not require self-similar or even steady behaviour, or that the scalar be passive.

A brief examination of the datasets listed in table 1 shows, unsurprisingly, that they are not quantitatively consistent with (3.3). Nevertheless, there are suggestive points of qualitative agreement. It has already been noted that all the observed transverse profiles have the off-axis maximum at $\eta = O(1)$ that is observed at Station A in figure 2(*b*) (refer to figure 1). Also, those papers presenting the axial variation of $\overline{c^2}/\theta_1^2$ (Becker *et al.* 1967; Birch *et al.* 1978; Fackrell & Robins 1982; Pitts & Kashiwagi 1984) show a maximum as in figure 2(*c*). However, the measured

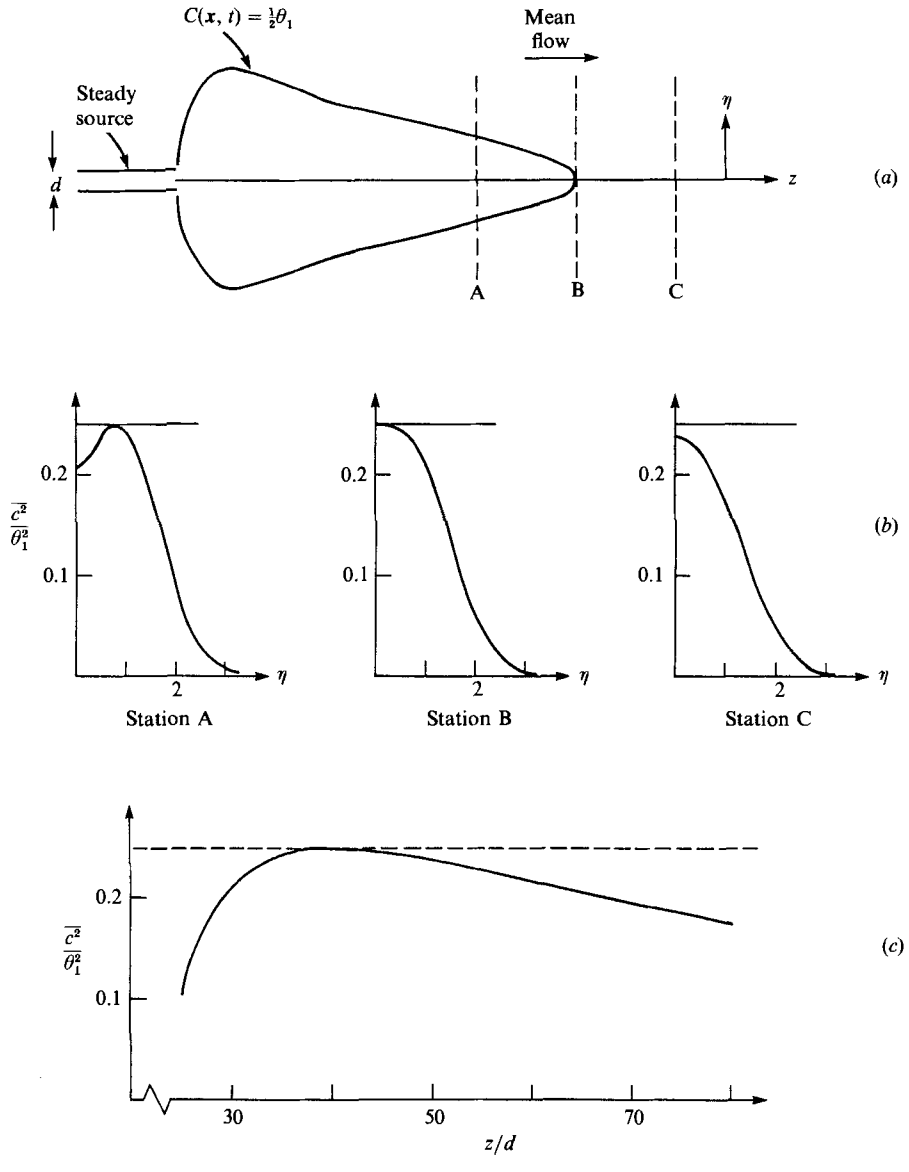

FIGURE 2. Schematic diagrams showing profiles of $\overline{c^2}/\theta_1^2$ given by (3.3) and (3.4): (*a*) geometry; (*b*) transverse profiles; (*c*) axial profile ($\eta = 0$). Note that $c^2/\theta_1^2 < \frac{1}{4}$ everywhere except on the surface indicated in (*a*), and that maxima in the profiles occur on crossing this surface.

maximum values of $\overline{c^2}/\theta_1^2$ are significantly less than 0.25, predicted by (3.3). For example, Becker *et al.* (1967, figure 7) observe a maximum value of $\overline{c^2}/\theta_1^2$ on the centreline of order 0.018, occurring when $C/\theta_1 \approx 0.77$ (not 0.5 as predicted by (3.3)), and $z/d \approx 13.2$. Figure 3 (Chatwin & Sullivan 1985, figure 3) illustrates typical quantitative deviations from (3.3) for transverse profiles.

3.1. *A hypothesis concerning the effects of molecular diffusion*

Molecular diffusion has several interrelated effects that invalidate (3.3) for real flows. Most fundamentally perhaps, the maximum concentration occurring at any point

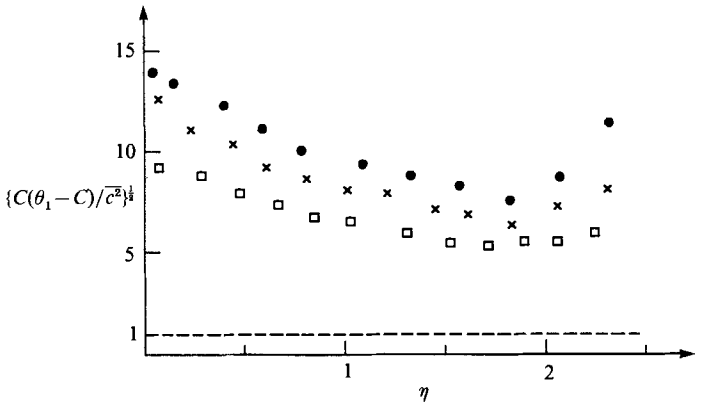

FIGURE 3. Data from Birch *et al.* (1978) □, ×, ● are for $z/d = 20, 30, 40$ respectively. Had the data agreed with (3.3), all points would be on the dashed line.

during any realization is less than the source concentration θ_1 by a factor that increases with z. Also molecular diffusion causes $\overline{c^2}$ to be dissipated in a way that depends not only on this reduction of the maximum concentration, but also on the statistical properties of the velocity field inasmuch as these determine the geometrical properties of the scalar-containing volumes emanating from the source. Not surprisingly, Professor George Batchelor was one of the first to identify the crucial importance of the latter point (Batchelor 1952), and its relationship to the dissipation of $\overline{c^2}$ was subsequently explored by him (Batchelor 1959; Batchelor *et al.* 1959) and many others. For well understood physical reasons that need not be repeated here, the magnitudes and variations of $C(\boldsymbol{x}, t)$ and $\overline{c^2}(\boldsymbol{x}, t)$ do not, however, depend (to any measurable degree at least) on the value of κ, the molecular diffusivity; this is consistent with the results of the datasets in table 1 for which there are wide variations in κ.

The effects of κ identified above occur on a very small lengthscale (of order equal to Batchelor's conduction cut-off length λ which is typically of magnitude 10^{-4}–10^{-3} m). Given this, it is natural to attempt to account for the effect of κ on the maximum concentration by replacing θ_1 in (3.3) by a local concentration scale $\alpha C_0(z)$, where $C_0(z)$ is the maximum mean concentration at downstream distance z defined in (2.1). In general, α will depend on factors like the type of flow and source geometry (but not on κ), and on $\boldsymbol{x}$ and t. However, in the statistically self-similar and steady conditions that apply for all the experimental data considered in this paper, α can depend only on similarity variables like η. But the further hypothesis will be made here that in such cases α is a constant of order unity. This is not only the simplest possible assumption but it has the physical justification (to be considered further in §5 below) that the evolution of the contaminant distribution is controlled by the large eddies of the velocity field so that only one concentration scale is relevant at any cross-section; this can obviously be taken to be a multiple of $C_0(z)$. In the first instance, therefore, the hypothesis is that (3.3) should be replaced by $\overline{c^2} = C(\alpha C_0 - C)$. However, this requires the value of α to account for both effects of κ described above, and this seems likely to be unreasonable in general. There is no conceptual difficulty in extending the hypothesis by including a reduction factor β in the equation for $\overline{c^2}$ to allow separately for dissipation. It will also be assumed (for the reasons given above in the case of α) that β is a constant independent of κ. Therefore the main work

of the remainder of this section will be to investigate whether the datasets in table 1 satisfy

$$\overline{c^2} = \beta C(\alpha C_0 - C), \tag{3.5}$$

with $C = C(z,\eta), \overline{c^2} = \overline{c^2}(z,\eta)$, and α and β constant.

Before giving the results of this investigation, it is helpful to mention two points that will be discussed in some detail in §5 below. Although (3.3) was derived from the explicit exact form (3.1) for the p.d.f. of $\Gamma(\boldsymbol{x}, t)$, no hypothesis has yet been made here concerning the p.d.f. in real flows that may lead to (3.5). Secondly, increasing attention (Sullivan 1984; Carn & Chatwin 1985; Chatwin & Sullivan 1987*a*, 1989*a*, *b*; Derksen & Sullivan 1987, 1989; Mole & Chatwin 1987; Mole 1989, 1990) is being given to the differences between actual and perceived (i.e. measured) values of $\overline{c^2}$ (and other statistical properties of $c(x,t)$) that may occur due to instrument smoothing; if there are such differences they may well affect the values of α and/or β, but they do not affect the data analysis and will be ignored in the remainder of this section.

3.2. *Comparison of* (3.5) *with the datasets in table* 1

After proposing (3.5) and drawing several of the graphs in figure 4 below, the authors discovered that Becker *et al.* (1967, figure 8) had shown that their data followed (3.5) 'highly accurately' with $\alpha \approx 1.31$ and $\beta \approx 0.156$. However, no physical explanation of its validity was attempted in that paper, and its status until now was purely empirical.

The procedure adopted to test whether (3.5) described the other datasets in table 1 was, first, to determine α by the location of the maximum in the (self-similar) transverse profile of $\overline{c^2}$; according to (3.5) this occurs when $C/C_0 = \frac{1}{2}\alpha$. Graphs of $\{C(\alpha C_0 - C)/\overline{c^2}\}^{\frac{1}{2}}$ against η were then drawn, and it can be seen from figure 4 that this quantity is a constant, within experimental error, for each dataset for η less than about 1.75. Thus each dataset in table 1 is consistent with (3.5), and the value of the constant is $\beta^{-\frac{1}{2}}$. Unfortunately all values of C and $\overline{c^2}$ had to be read from the graphs in the published papers and this unsatisfactory procedure accounts for a substantial proportion of the scatter in the graphs in figure 4; these reading errors are relatively greatest at the larger values of η where both $\overline{c^2}$ and $C(\alpha C_0 - C)$ approach zero.

Table 2 gives the values of α and β for all the datasets. These values are very comparable with those given for some of the experiments by Chatwin & Sullivan (1987*a*), and obtained by a least-squares procedure.

Although the method used in obtaining figure 4 artificially highlights measurement, and graph-reading, errors in the low values of C and $\overline{c^2}$ at higher values of η, figure 5 suggests that these are likely to be of little practical significance. The simple, and physically based, equation (3.5) provides at least as good a fit (and arguably better) to the data of Fackrell & Robins (1982) as a complicated formula due to Wilson, Robins & Fackrell (1982), viz.

$$\overline{c^2} = 0.784\{\exp[-\ln 2\,|\eta - 0.6|^{1.7}] - 0.6\exp[-\ln 2\,|\eta + 0.6|^{1.7}]\}. \tag{3.6}$$

This was based on a source–sink image system hypothesis, and all the numbers in (3.6) had to be determined from the data.

3.3. *Comments on experiments by Nakamura, Sakai & Miyata* (1987)

It will be observed that the numbers in table 2 satisfy $1 < \alpha < 2$ and $\beta < 1$, and further interpretation of the values of these parameters will be given later. However, a single comment about α is appropriate here. It follows from (3.5) that

$$\overline{c^2} = \beta[\tfrac{1}{4}\alpha^2 C_0^2 - (C - \tfrac{1}{2}\alpha C_0)^2]. \tag{3.7}$$

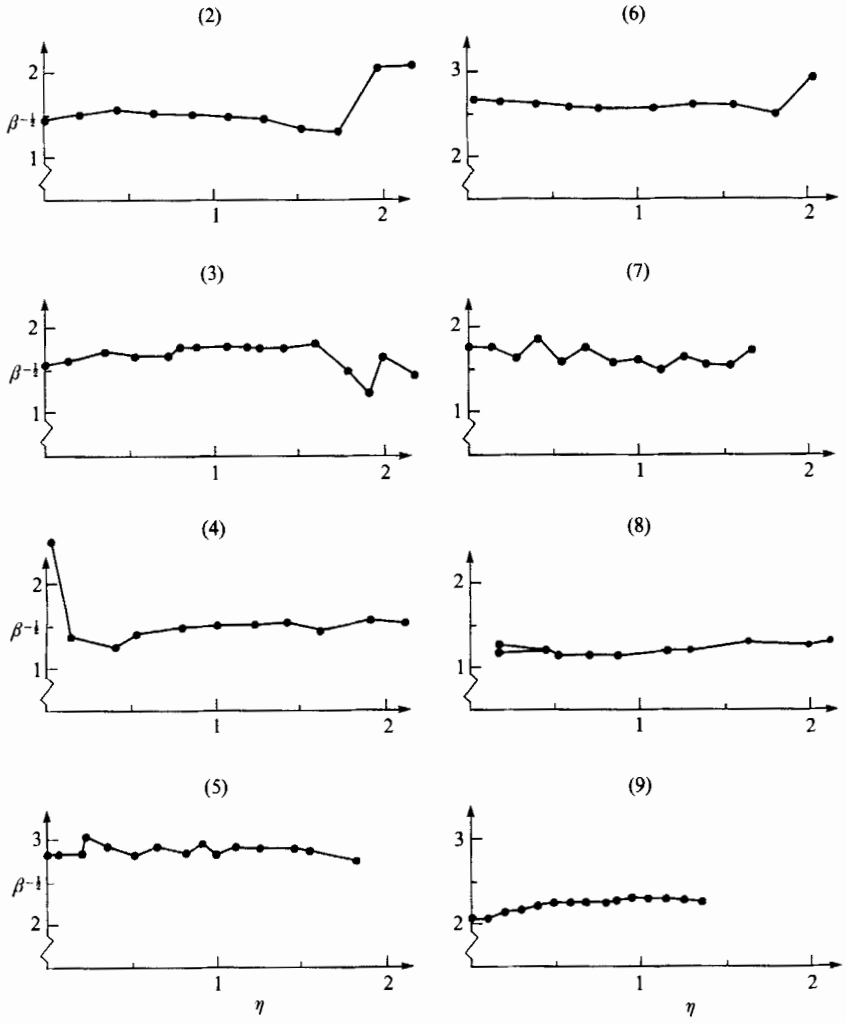

FIGURE 4. Graphs of $\beta^{-\frac{1}{2}} = \{C(\alpha C_0 - C)/\overline{c^2}\}^{\frac{1}{2}}$ versus η for the datasets in table 1, where α and β are defined in (3.5). The numbers on the graphs, e.g. (2), correspond with those in table 1.

NO.	α	β	NOTES
(1)	1.31	0.16	Values from empirical relationship in paper
(2)	1.17	0.46	
(3)	1.16	0.34	
(4)	1.09	0.46	Data for $z/d = 102$
(5)	1.24	0.12	
(6)	1.27	0.14	Data for $z/d = 40$
(7)	1.52	0.37	
(8)	1.35	0.72	Data for $z/H = 5.00, 5.92$
(9)	1.15	0.20	

TABLE 2. Values of α and β for table 1 datasets

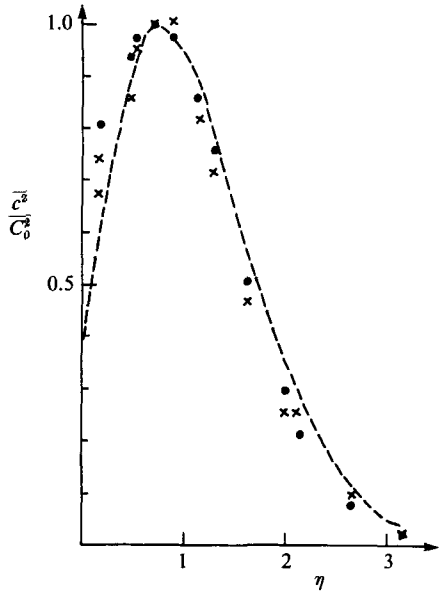

FIGURE 5. Comparison of (3.5) (●) with boundary-layer data from Fackrell & Robins (1982) (×), where c_0^2 is the maximum value of $\overline{c^2}$. The dashed curve is (3.6).

Since $C \leqslant C_0$ everywhere at any fixed cross-section, an off-axis maximum in the transverse profile of $\overline{c^2}$ occurs only if $\alpha < 2$. There is no fundamental physical reason why this condition should always be satisfied and, indeed, there is good experimental evidence that it is not. Data on the dispersion of dye in grid-generated water turbulence taken with a light absorption probe by Nakamura, Sakai & Miyata (1987) showed no off-axis maximum in the transverse profiles of $\overline{c^2}$, although these were 'nearly' self-similar. It was noted that this observation contradicted the results of Gad-el-Hak & Morton (1979), no. (7) in table 1 and figure 4. The main point of interest here is that Nakamura *et al.* (1987) showed (their figure 16) that their profiles of $\overline{c^2}$ could be fitted well by a curve whose equation (obtained by rearranging their equation (31)) is exactly (3.5) with $\alpha = 3$ (their P is the present α) and $\beta = 1$. No off-axis maximum of $\overline{c^2}$ therefore occurs.

Two further points about these experiments are relevant. Nakamura *et al.* (1987) attributed the differences between their results and those of Gad-el-Hak & Morton (1979) to the fact that their fluctuating concentration field was highly intermittent everywhere unlike that recorded by Gad-el-Hak & Morton (1979), and it would be very interesting to know whether this difference in intermittency behaviour was genuine, or due to differences in the degree of instrument smoothing. It was also shown that the observed values of $\overline{c^2}$ were strongly dependent on the source geometry consistent with the theoretical explanation by Chatwin & Sullivan (1979).

4. Higher moments

Although (3.5) is simple, it does appear to describe the data on $\overline{c^2}$ remarkably accurately, and – with this encouragement – it is natural to extend the ideas of §3 to higher moments, including shape parameters like skewness and flatness factor (or kurtosis).

The moment generating function $M(s)$ is defined by

$$M(s) = 1 + \sum_{n=2}^{\infty} \overline{c^n}\left(\frac{s^n}{n!}\right) = \int_0^{\infty} \mathrm{e}^{(\theta - C)s}\, p\, \mathrm{d}\theta. \tag{4.1}$$

Applying this to the basic p.d.f. (3.1) on which (3.5) was based gives

$$1 + \sum_{n=2}^{\infty} \overline{c^n}\left(\frac{s^n}{n!}\right) = \pi\, \mathrm{e}^{(\theta_1 - C)s} + (1-\pi)\, \mathrm{e}^{-Cs}, \tag{4.2}$$

and then, on expanding the right-hand side and eliminating π using (3.2),

$$\overline{c^n} = \frac{C}{\theta_1}(\theta_1 - C)^n + (-1)^n\left(1 - \frac{C}{\theta_1}\right)C^n. \tag{4.3}$$

It is elementary to check that (4.3) vanishes as $\theta_1 \to 0$ (there is then no scalar, and note that $0 \leqslant C \leqslant \theta_1$) and when $C = \theta_1$ (all the fluid is then occupied by scalar, i.e. $\pi = 1$ everywhere).

The hypothesis made in §3 will be extended in the obvious way to all n by replacing, in (4.3), (*a*) θ_1 by the local concentration scale αC_0 and (*b*) equality by proportionality. Thus (4.3) becomes

$$\overline{c^n} \propto \frac{C_0^n}{\alpha}\{x(\alpha - x)^n + (-1)^n(\alpha - x)x^n\}, \tag{4.4}$$

where

$$x = C/C_0. \tag{4.5}$$

In particular

$$\left.\begin{aligned} \overline{c^2} &= \beta C_0^2 f_2(x), \quad f_2(x) = x(\alpha - x), \\ \overline{c^3} &= \gamma C_0^3 f_3(x), \quad f_3(x) = x(\alpha - x)(\alpha - 2x), \\ \overline{c^4} &= \delta C_0^4 f_4(x), \quad f_4(x) = x(\alpha - x)(\alpha^2 - 3\alpha x + 3x^2), \end{aligned}\right\} \tag{4.6}$$

where β, γ, δ are the constants of proportionality for $n = 2, 3, 4$ respectively, and the first of (4.6) is the same as (3.5). The shape parameters S (skewness) and F (flatness factor) then satisfy†

$$\left.\begin{aligned} S &= \frac{\overline{c^3}}{(\overline{c^2})^{\frac{3}{2}}} \Rightarrow S = \frac{\gamma}{\beta^{\frac{3}{2}}} f_S(x), \quad f_S(x) = \frac{(\alpha - 2x)}{\{x(\alpha - x)\}^{\frac{1}{2}}}, \\ F &= \frac{\overline{c^4}}{(\overline{c^2})^2} \Rightarrow F = \frac{\delta}{\beta^2} f_F(x), \quad f_F(x) = \frac{(\alpha^2 - 3\alpha x + 3x^2)}{x(\alpha - x)}. \end{aligned}\right\} \tag{4.7}$$

Despite the extreme simplicity of the physical model underlying (4.4), (4.6) and (4.7), these results have surprisingly rich structure. Some features of this structure, obtainable by elementary mathematics, are given in table 3. This structure is also shown by figure 6 (except for $\alpha > 3 + \sqrt{3}$ for which there are no known data).

4.1. *Comparison with data*

Measurements of the higher moments are less common than those of C and $\overline{c^2}$, and they are also more difficult, partly because of enhanced sampling errors. Kendall &

† The formulae corresponding to (4.7) that follow from (4.3), rather than (4.4), are given by Chevray & Tutu (1977).

<table>
<tr><td>$1 < \alpha < 3-\sqrt{3}\ (\approx 1.268)$</td><td>$3-\sqrt{3} < \alpha < 2$</td><td>$2 < \alpha < 3+\sqrt{3}\ (\approx 4.732)$</td><td>$\alpha > 3+\sqrt{3}$</td></tr>
<tr><td colspan="2">All odd moments are zero when $x = x_0 = \frac{1}{2}\alpha$
All even moments have a stationary point when $x = x_0$
(max. for $n = 2$; min. for all other even n)</td><td colspan="2">These features are absent since $x < x_0$ everywhere</td></tr>
<tr><td colspan="3">f_3 has a max. at $x = x_1 = \frac{1}{6}(3-\sqrt{3})\alpha\ (\approx 0.211\alpha)$ of value $\frac{\sqrt{3}}{18}\alpha^3\ (\approx 0.096\alpha^3)$</td><td>No max. in f_3 since $x < x_1$ everywhere</td></tr>
<tr><td>f_3 has a min. at $x = x_{-1} = \frac{1}{6}(3+\sqrt{3})\alpha\ (\approx 0.789\alpha)$ of value $-\frac{\sqrt{3}}{18}\alpha^3$</td><td colspan="3">No min. in f_3 since $x < x_{-1}$ everywhere</td></tr>
<tr><td colspan="3">f_4 has a max. at $x = x_1$ of value $\frac{1}{12}\alpha^4\ (\approx 0.083\alpha^4)$</td><td rowspan="2">No max. in f_4 since $x < x_1$ everywhere</td></tr>
<tr><td>f_4 has a max. at $x = x_{-1}$ of value $\frac{1}{12}\alpha^4$</td><td colspan="2">Feature absent since $x < x_{-1}$ everywhere</td></tr>
<tr><td colspan="4">The skewness (f_S) is a monotonically decreasing function of x; $f_S \to \infty$ as $x \to 0+$</td></tr>
<tr><td colspan="2">f_S is zero when $x = x_0$</td><td colspan="2">Feature absent since $x > x_0$ everywhere</td></tr>
<tr><td colspan="4">The flatness factor (f_F) $\to \infty$ as $x \to 0+$</td></tr>
<tr><td colspan="2">f_F has a min. when $x = x_0$ of value 1</td><td colspan="2">Feature absent since $x < x_0$ everywhere</td></tr>
</table>

TABLE 3. Features of the behaviour of the higher moments, where $x = C/C_0$

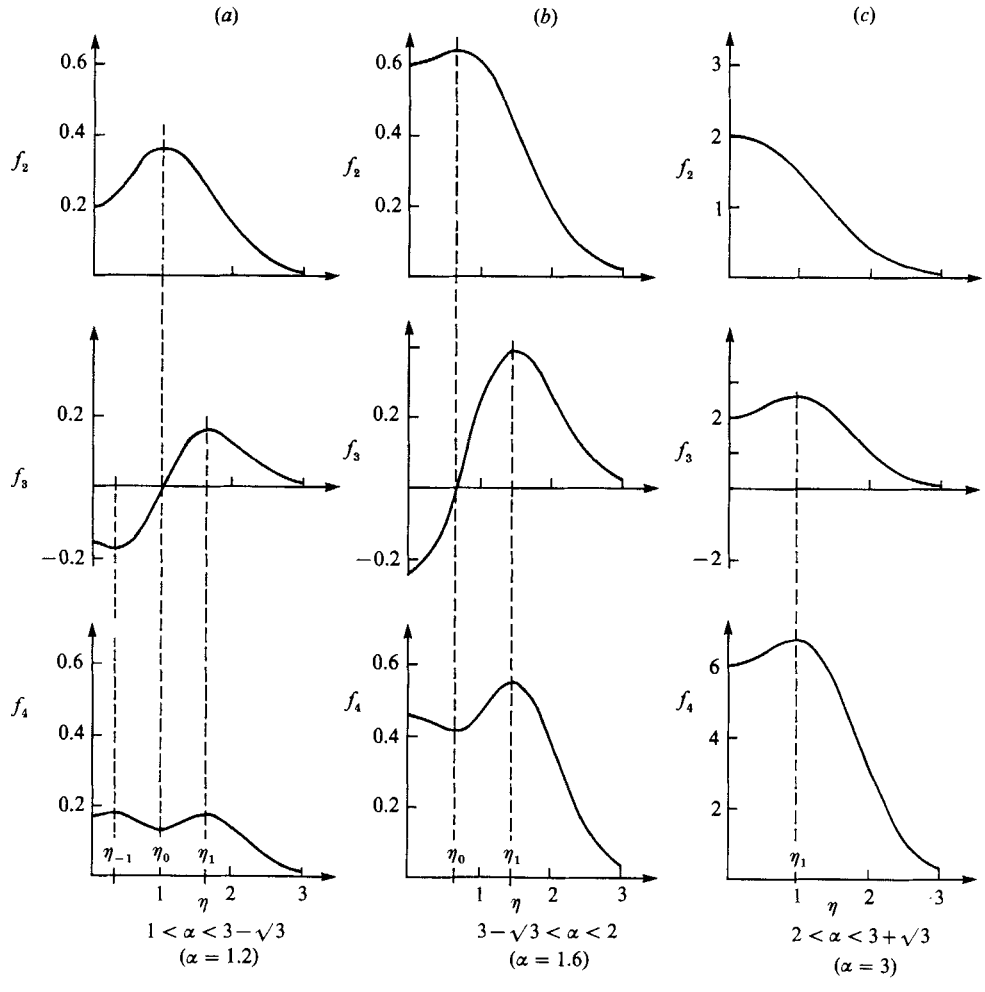

FIGURE 6(a–c). For caption see facing page.

Stuart (1977, p. 249) emphasize how rapidly the standard errors of measured moments increase with order. Sreenivasan (1981) notes the slow convergence of measurements of S, while Antonia, Chambers & Elena (1983*b*) point out that there is a larger scatter in the determination of an odd moment when its magnitude is small. Figures 6 and 7 of Pitts & Kashiwagi (1984) illustrate how large the scatter can be in practice for S and F. Despite such problems, available data on the higher moments are remarkably consistent with certain properties of the theoretical predictions (4.6) and (4.7).

In the first place, for cases for which there are appropriate measurements, the transverse profiles of S and F become self-similar. These include a plane wake (LaRue & Libby 1974; Sreenivasan 1981), a heated round jet (Antonia *et al.* 1975; Chevray & Tutu 1977), a round methane jet exhausting into air (Birch *et al.* 1978; Pitts & Kashiwagi 1984), a thermal mixing layer (LaRue & Libby 1981) and a reacting jet diffusion flame (Drake, Shyy & Pitz 1985). In all these examples, the centreline ($\eta = 0$) value of S is negative, the profile of F has an off-axis minimum and the values of both S and F are very large and positive at values of η greater than about 2, entirely consistent with (4.7) – see table 3 and figure 6(*d*).

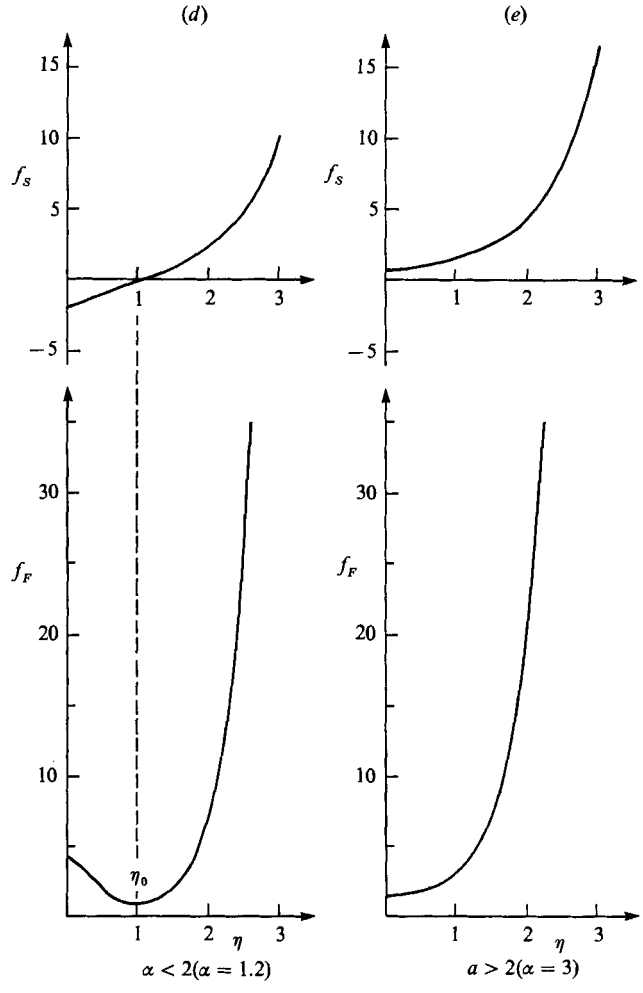

FIGURE 6. The shapes of the first three moments, (*a*), (*b*), (*c*), and the shape parameters, (*d*), (*e*), where the functions plotted are defined in (4.6) and (4.7). In order to draw the graphs it has been assumed – see (3.4) – that $x = C/C_0 = e^{-\frac{1}{2}\eta^2}$, and particular values of α have been chosen as indicated, but the shapes are not sensitively dependent on these arbitrary selections. Collectively the graphs show the complete behaviour (except for magnitudes) that can occur for practical values of α. The notation η_i on the sketches corresponds to x_i in table 3, i.e. $x_i = e^{-\frac{1}{2}\eta_i^2}$ $(i = 0, \pm 1)$.

Moreover the zero of S always coincides (approximately or better) with the minimum of F and – in cases where profiles of $\overline{c^2}$ are also given – with the maximum of $\overline{c^2}$. This agrees with a basic premise of the hypothesis in the present paper, namely the existence of the local concentration scale αC_0, where the constant α has the same value for all moments as in (4.4) and (see table 3) the maximum of $\overline{c^2}$, the zero of S, and the minimum of F, occur where $\eta = \eta_0$, i.e. $x = x_0 = \frac{1}{2}\alpha$. (It follows that for all the data quoted above the value of α is less than 2.) From (4.4) it is straightforward to show that, when $\alpha < 2$, these properties of S and F extend to shape parameters of still higher order. In particular all odd-order shape parameters $\overline{c^{2n+1}}/(\overline{c^2})^{n+\frac{1}{2}}$ are zero, and all even-order shape parameters $\overline{c^{2n}}/(\overline{c^2})^n$ have a minimum for $n > 1$, when $\eta = \eta_0$, $x = x_0 = \frac{1}{2}\alpha$. Qualitatively the profiles of all odd and even parameters are like those of f_S and f_F respectively in figure 6 (*d*), although the approach to infinity with increasing

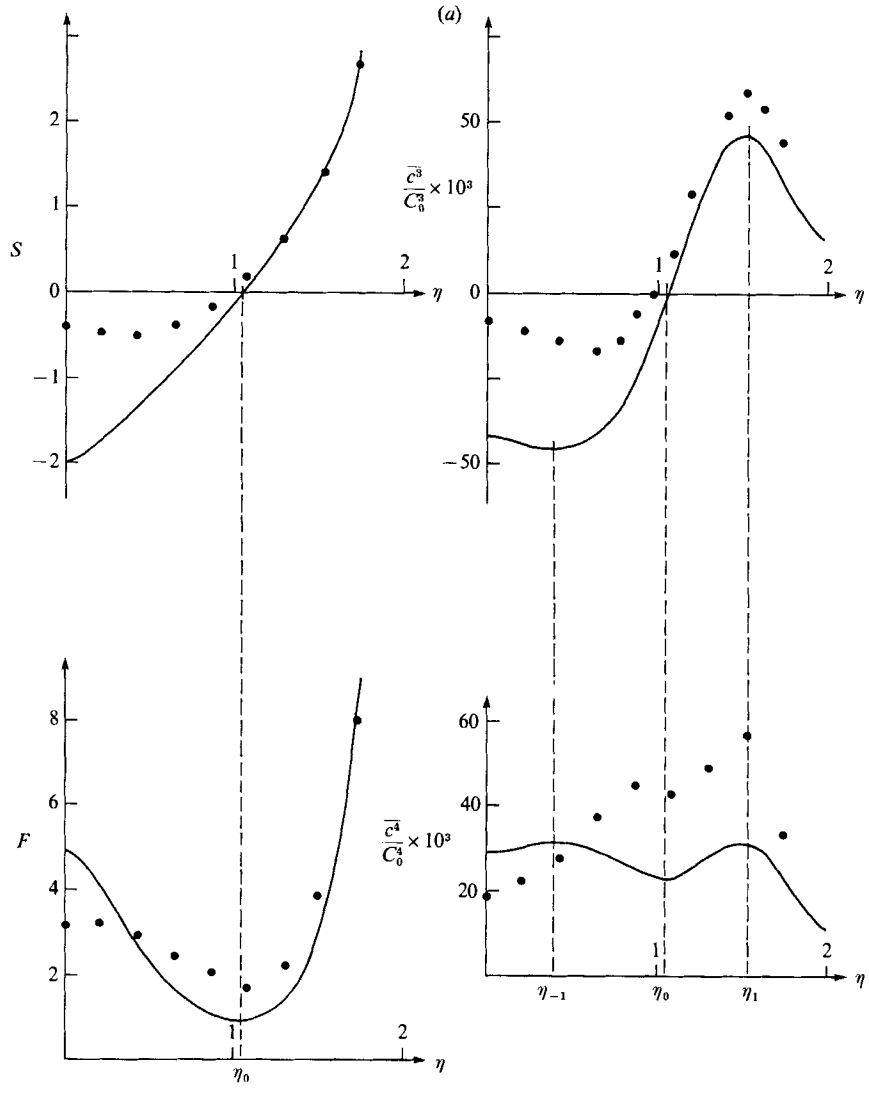

FIGURE 7(*a*). For caption see p. 548.

η is more rapid the higher the order. These predictions are consistent up to order 8 with measurements in a round jet by Antonia & Sreenivasan (1976); further (and despite the difficulties of measurement) the numerical values that they report are shown to agree with (4.4) to much better than an order of magnitude by Chatwin & Sullivan (1987*b*). Antonia *et al.* (1983*b*) present other empirical evidence that supports these predictions and observe that they hold to good approximation in several different shear flows, again consistent with the underlying hypothesis of the present paper that (4.4) is universally applicable. In the same paper Antonia *et al.* (1983*b*) show that measurements from several different shear flows appear to collapse on power-law graphs of the form

$$\frac{\overline{c^4}}{(\overline{c^2})^2} \propto \left\{\frac{\overline{c^6}}{(\overline{c^2})^3}\right\}^m \quad \text{and} \quad \frac{\overline{c^6}}{(\overline{c^2})^3} \propto \left\{\frac{\overline{c^8}}{(\overline{c^2})^4}\right\}^n, \tag{4.8}$$

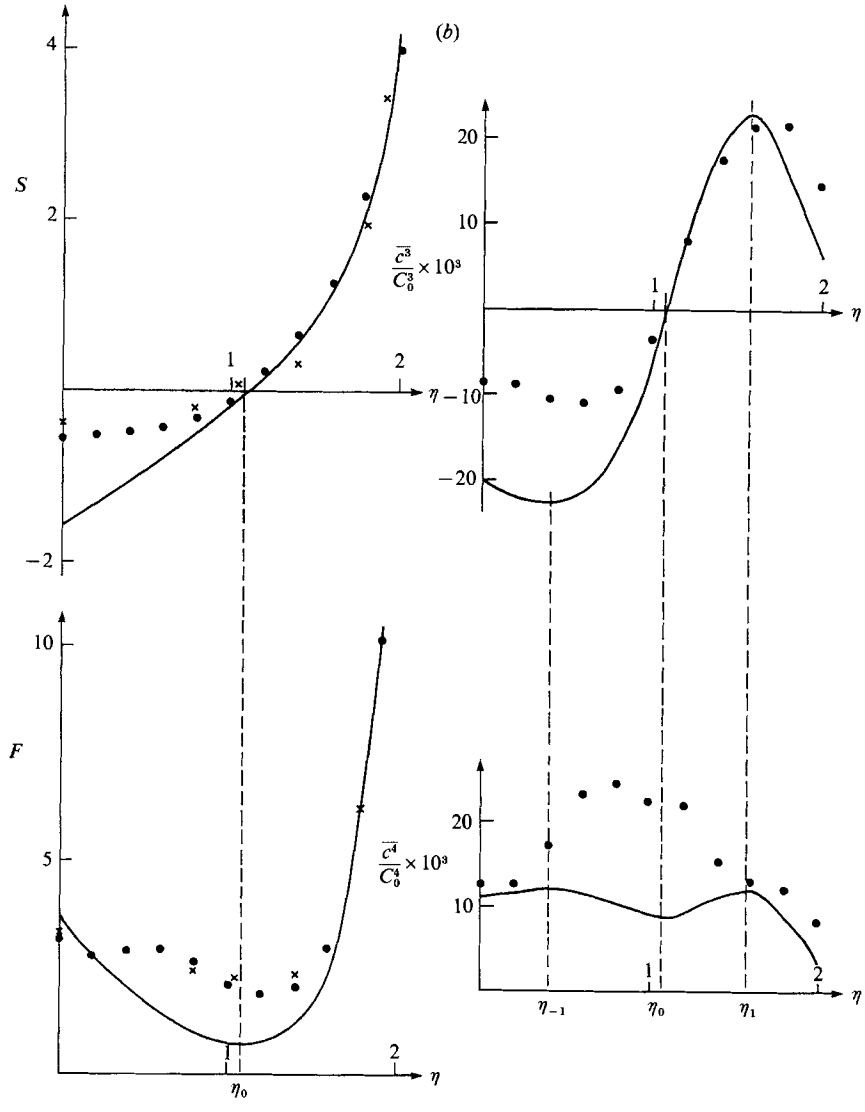

FIGURE 7(*b*). For caption see p. 548.

where $m \approx 0.4$ and $n \approx 0.65$ are the same for all the flows. It is of interest to note that, over the relevant parameter ranges, the predictions from (4.4) are well approximated by such relationships with $m \approx 0.47$ and $n \approx 0.68$, reasonably near the experimental values. While the numerical agreement is supportive of (4.4), the power laws themselves are unlikely to have any physical meaning, being due merely to arithmetical chance.

Sreenivasan (1981 – plane wake) and Browne, Antonia & Chambers (1984 – plane jet) show the axial variation of S and F in the region before similarity has been established. While the approach of S to its negative value at $\eta = 0$ is different in the two flows – in the plane wake $S|_{\eta=0}$ is positive for $z/d < 78$ and negative thereafter whereas in the plane jet it is positive for $8 < z/d < 14$ and negative elsewhere – a zero

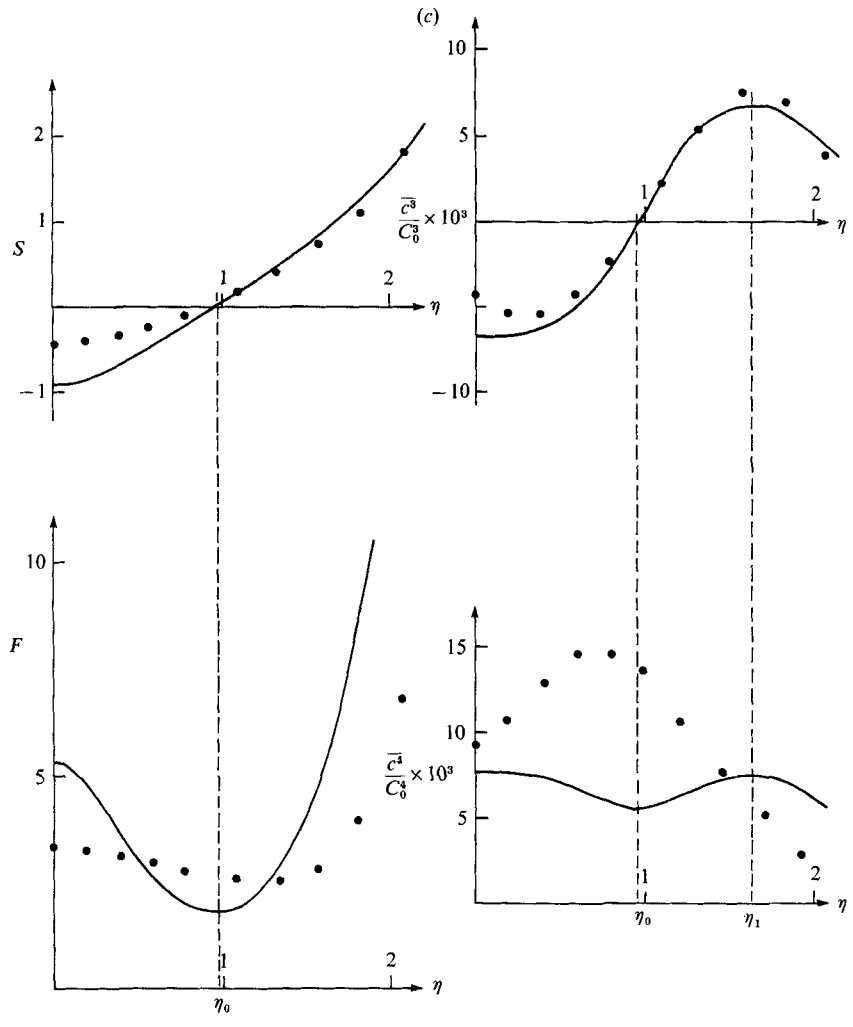

FIGURE 7. Comparison of three datasets with (4.6) and (4.7). The solid curves are theoretical and the solid circles are obtained from the data in the way described in the text. (*a*) LaRue & Libby (1974); (*b*) Antonia *et al.* (1975); ×, data from Antonia & Sreenivasan (1976). (*c*) Birch *et al.* (1978).

of S coincides with a minimum of F in both cases. In the plane jet this position is also one where the moments of order 5 and 7 vanish. Of course (4.4) does not apply here since self-similarity has not been established, but the same phenomena are predicted by (4.3). It therefore seems that the transition from (4.3) to (4.4) as z/d increases, due entirely to κ, is one in which these robust properties are preserved. Figure 12 of Browne *et al.* (1984) shows, however, that there are great changes in the shape of the p.d.f. of concentration in this transition region.

Quantitative comparisons of three datasets with (4.6) and (4.7) are shown in figure 7. In each case data for S and F were read from the graphs in the paper; these were then used to estimate $\overline{c^3}$ and $\overline{c^4}$ by using the readings of $\overline{c^2}$ already employed in figure 4. (None of the papers gives profiles of $\overline{c^3}$ and $\overline{c^4}$.) Smooth curves of best fit were drawn by eye to the data thus obtained, and the solid circles in figure 7 are readings

Dataset	γ	δ
LaRue & Libby (1974), plane wake	0.3	0.2
Antonia *et al.* (1975), round jet with coflowing stream	0.15	0.08
Birch *et al.* (1978), round methane jet	0.034	0.035

TABLE 4. Values of γ and δ for the theoretical curves in figure 7

from these curves. The values of γ and δ shown in table 4 were chosen as those that appeared to give as reasonable agreement as possible between the (modified) data points and the theory of (4.6) and (4.7). The judgement was based on visual comparison only, with emphasis on overall shape and order of magnitude. The values of α and β used in this process and in drawing the curves in figure 7 were, of course, those obtained earlier and given in table 2. It will be seen that the comparisons in figure 7 are generally less good than those involving $\overline{c^2}$ alone; nevertheless there is reasonable agreement for the S, F and $\overline{c^3}/C_0^3$ profiles, given the difficulties of (*a*) making the measurements, and (*b*) reading accurately from the published graphs. These difficulties, and the procedure used to interpolate to the data, could account for the principal difference in all three cases between theory and experiment, namely that the data are flatter in the central portion than (4.6) and (4.7) predict. The $\overline{c^4}/C_0^4$ comparison is less satisfactory, but it is for this profile that the difficulties referred to will have greatest effect. (These comments on figure 7 apply also to other comparisons between the same data and the same theory given by Chatwin & Sullivan 1987*b*.)

5. Discussion

On the basis of the evidence presented above, the basic hypothesis of this paper would seem to merit further experimental investigation. Its most attractive features are its simplicity, and its apparent applicability to all shear flows. (Irrespective of whether the *present* hypothesis proves, ultimately, to be correct, the similarity of the comparisons, for different shear flows, between theory and experiment, apparent from figures 4 and 7 for example, suggests that there is *some* hypothesis applicable to all flows.) The remainder of this paper comments on some important questions raised by the work above.

5.1. *The probability density function*

Since a p.d.f. is determined by the set of its moments (except for some pathological and unpractical cases), self-similar structure of $\overline{c^n}$ for all n implies that $p(\theta;\boldsymbol{x})$ is also self-similar, where – as the notation indicates – attention will be restricted to statistically steady situations with the p.d.f. independent of t. Mathematically the argument requires some uniformity conditions on the rapidity of approach to self-similarity of $\overline{c^n}$, but this point is never likely to have practical importance because $p(\theta;\boldsymbol{x})$ is determinable effectively from a small number of its moments (Birch *et al.* 1978; Derksen & Sullivan 1989). Many workers assume such self-similarity without comment, but Sreenivasan (1981; plane wake) and Dowling & Dimotakis (1988; round jet) explicitly measure the approach to self-similarity. The latter authors note decreased statistical convergence as η increases, i.e. near the edges of the jet.

It is shown in Chatwin & Sullivan (1989*a*) that $p(\theta;x)$ has the exact representation (cf. (3.1) above):

$$p(\theta;x) = \pi_0(x)\psi(\theta;x) + \{1-\pi_0(x)\}\varphi(\theta;x), \tag{5.1}$$

where $\pi_0(x)$ is a proposed new measure of the intermittency factor. When the dispersing scalar has uniform concentration θ_1 on release, as in all the experiments discussed in this paper,

$$\pi_0(x) = \frac{C(x)}{\theta_1}, \tag{5.2}$$

where $\psi(\theta;x)$ and $\varphi(\theta;x)$ are themselves p.d.f.s. They are defined in relation to the (hypothetical) ensemble of dispersion experiments which is identical in all respects to the real one *except* that there is no molecular diffusion. If $\Gamma_0(x,t)$ denotes the scalar concentration in this hypothetical ensemble, then ψ and φ are the p.d.f.s of Γ (the real concentration) conditional, respectively, on $\Gamma_0 = \theta_1$ and $\Gamma_0 = 0$, and have simple physical interpretations. For example ψ is the p.d.f. of concentration in those fluid particles emanating from the source. In the absence of molecular diffusion the p.d.f. is given by (3.1) so the manner in which ψ and φ differ from delta functions is entirely due to molecular diffusion.

From (5.1) and (5.2) self-similarity of $p(\theta;x)$ is ensured far enough downstream (since $\pi_0(x)\to 0$ as $|x|\to\infty$) provided $\varphi(\theta;x)$ becomes self-similar, and then $p \approx \varphi$. However, the self-similarity of $p(\theta;x)$ observed in a round jet by Dowling & Dimotakis (1988) appears essentially to be established on the centreline at only 20 (or so) jet diameters downstream where π_0 is as high as 0.21. The following argument suggests why the effects of molecular diffusion may cause self-similarity to be established more rapidly in practice than is ensured by (5.1) and (5.2).

Consider the set of fluid particles that go through the point with position vector x. As indicated schematically in figure 8, this set comprises two mutually exclusive subsets. Choose η_1 to have any fixed value of about 2. Then the trajectory of any one fluid particle will have crossed $\eta = 0$ more recently than $\eta = \eta_1$ (set 0), or vice versa (set 1). (For x far enough from the source, those particles that have crossed neither $\eta = 0$ nor $\eta = \eta_1$ will be a negligible proportion.) For set 0, suppose the crossing occurs at $z = Z$, and let $q_0(\zeta)$ be the p.d.f. of Z, i.e.

$$\text{prob}\,(Z \leqslant z_0) = \int_{-\infty}^{z_0} q_0(\zeta)\,\mathrm{d}\zeta \tag{5.3}$$

for any z_0; define $q_1(\zeta)$ analogously for set 1. The dependence of q_0 and q_1 on x is not shown explicitly, nor known, but certain features are obvious. Thus as η (the non-dimensional transverse coordinate of x) approaches zero, q_0 approaches $\delta(\zeta-z)$, where z is the axial coordinate of x; in general q_0 will be non-zero over a range of values of ζ whose effective width, say Δ, tends to zero as $\eta\to 0$. Corresponding comments apply to q_1.

It will now be assumed that the effects of molecular diffusion are significant only over axial lengthscales of order z and, correspondingly, can be neglected over lengthscales of order Δ. While it is clear that this assumption will be best near $\eta = 0$ or $\eta = \eta_1$, its validity in general follows from the facts that the statistics of the fluid particle trajectories are determined by the fast (and self-similar) large-scale motions in the shear flow, and that, as $|x|$ increases, the instantaneous concentration gradients over the bulk of the flow reduce so that molecular mixing becomes

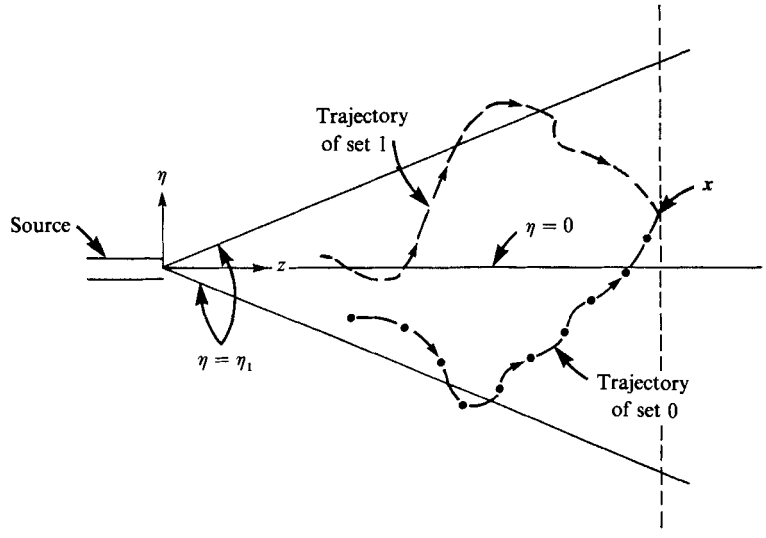

FIGURE 8. Sketch illustrating schematically the two sets of trajectories: 0 (–●–●) and 1 (– – –).

increasingly slower. Therefore, to good approximation, the value of $\Gamma(\boldsymbol{x},t)$ can be taken to be its value at its last crossing of $\eta = 0$ or $\eta = \eta_1$ (as appropriate). Hence

$$p(\theta;\boldsymbol{x}) \approx \int_{\Delta} p(\theta;0,\zeta)\, q_0(\zeta)\,\mathrm{d}\zeta + \int_{\Delta} p(\theta;\eta_1,\zeta)\, q_1(\zeta)\,\mathrm{d}\zeta, \tag{5.4}$$

where the use of the symbol Δ denotes integration from $z-\Delta$ to z.

It is now convenient to express $p(\theta;0,\zeta)$ and $p(\theta;\eta_1,\zeta)$ in the forms

$$\left.\begin{aligned} p(\theta;0,\zeta) &= \frac{\chi_0(\tau;0,\zeta)}{C_0(\zeta)}, \qquad \tau = \frac{\theta}{C_0(\zeta)}; \\ p(\theta;\eta_1,\zeta) &= \frac{\chi_1(\tau;\eta_1,\zeta)}{C(\eta_1,\zeta)}, \qquad \tau = \frac{\theta}{C(\eta_1,\zeta)}, \end{aligned}\right\} \tag{5.5}$$

where, using the basic property of $p(\theta;\boldsymbol{x})$ and the definition of C in (1.2),

$$\int_0^\infty \chi_0\,\mathrm{d}\tau = \int_0^\infty \chi_1\,\mathrm{d}\tau = \int_0^\infty \tau\chi_0\,\mathrm{d}\tau = \int_0^\infty \tau\chi_1\,\mathrm{d}\tau = 1. \tag{5.6}$$

The moments of Γ about zero, i.e. $E\{\Gamma^n\}$ – where E denotes expectation in standard statistical terminology – satisfy

$$E\{\Gamma^n\} = \int_0^\infty \theta^n\, p(\theta;\boldsymbol{x})\,\mathrm{d}\theta, \tag{5.7}$$

so that, using (5.5) and (5.6),

$$E\{\Gamma^n\} = \int_{\Delta} C_0^n(\zeta)\, q_0(\zeta)\left[\int_0^\infty \tau^n\chi_0\,\mathrm{d}\tau\right]\mathrm{d}\zeta + \int_{\Delta} C^n(\eta_1,\zeta)\, q_1(\zeta)\left[\int_0^\infty \tau^n\,\chi_1\,\mathrm{d}\tau\right]\mathrm{d}\zeta. \tag{5.8}$$

Since η_1 has been chosen so that $C_0^n(\zeta) \gg C^n(\eta_1, \zeta)$ for large enough ζ, and since χ_0 and χ_1 are of order 1, it follows that

$$E\{\Gamma^n\} \approx \int_A C_0^n(\zeta)\, q_0(\zeta) \left[\int_0^\infty \tau^n \chi_0 \, \mathrm{d}\tau\right] \mathrm{d}\zeta, \tag{5.9}$$

for large enough z. Moreover, the scaling of $p(\theta; 0, \zeta)$ in (5.5) is very likely to ensure that

$$\left[\int_0^\infty \tau^n \chi_0 \, \mathrm{d}\tau\right]$$

is, at worst, an extremely slowly varying function of ζ; thus (5.9) can be simplified further to

$$E\{\Gamma^n\} \approx \chi_n \int_A C_0^n(\zeta)\, q_0(\zeta) \, \mathrm{d}\zeta, \tag{5.10}$$

where

$$\chi_n = \int_0^\infty \tau^n \chi_0 \, \mathrm{d}\tau, \tag{5.11}$$

and can be taken as constant.

In the interests of algebraic simplicity, these arguments have been presented in terms of $E\{\Gamma^n\}$ rather than the central moment $E\{(\Gamma - C)^n\} = \overline{c^n}$ considered earlier. However, there is a straightforward algebraic relationship (Kendall & Stuart 1977, p. 58) between the two sets of moments from which it is easy to see, in particular, that one set of moments is self-similar if and only if the other set is. Reference to (5.10) shows that $E\{\Gamma^n\}$ depends on $\boldsymbol{x}$ only via the dependence of q_0 on $\boldsymbol{x}$, and this dependence was discussed above. Hence both sets of moments – and therefore $p(\theta; \boldsymbol{x})$ – are self-similar provided only that the single function q_0 is a self-similar function of $\boldsymbol{x}$ (not necessarily of ζ). While there is no proof that this is so, nor any data, it does not seem to be an unreasonable requirement (given the observed self-similarity of the low-order moments). In that case the eventual structure of $p(\theta; \boldsymbol{x})$ is essentially dominated by events on the line $\eta = 0$. Physically the arguments show that self-similarity of $p(\theta; \boldsymbol{x})$ occurs because of the self-similarity of the fast large-scale eddies in all the flows under consideration, together with the slow process of complete mixing caused by molecular diffusion; a further consequence (already assumed in the earlier data analysis) is that the scaling factors $\alpha, \beta, \gamma, \delta, \ldots$ ought to be constant. (For completeness it might also be noted that a lack of coincidence between the contaminant source and the fluid momentum source, e.g. a jet, may delay – but is unlikely to prevent – the onset of self-similar structure of $p(\theta; \boldsymbol{x})$ and other concentration fluctuation statistics.) It was noted earlier, following (5.1), that $p(\theta; \boldsymbol{x})$ must eventually approach $\varphi(\theta; \boldsymbol{x})$, the p.d.f. of concentration in those fluid particles *not* originating from the source, and therefore initially devoid of scalar. This occurs only because such fluid particles are entrained into the core of the flow by the large eddies (where their volume eventually dominates over fluid particles originating from the source) but self-similarity occurs only when the much slower process of molecular transfer from the source particles is complete.

The above argument does not deal with the dependence of the p.d.f. on θ once self-similarity has been established. However, for completeness, it can be recorded that Chatwin & Sullivan (1987*b*) and Derksen & Sullivan (1989) showed that, for many of the shear flows considered in this paper, $p(\theta; \boldsymbol{x})$ could be quite well described by the family of Beta distributions (Kendall & Stuart 1977, p. 162). This family has also

Dataset	$\beta^{\frac{1}{2}}$	$\gamma^{\frac{1}{3}}$	$\delta^{\frac{1}{4}}$
LaRue & Libby (1974)	0.68	0.67	0.67
Antonia *et al.* (1975)	0.58	0.53	0.53
Birch *et al.* (1978)	0.37	0.32	0.43

TABLE 5. Test of (5.12) for the datasets of table 4 and figure 7

been used by other workers, including Effelsberg & Peters (1983) and Drake *et al.* (1985).

5.2. *The values of* β, γ, δ, ...

The quantity β was first introduced in (3.5) to allow for possible overall reduction of measured values of $\overline{c^2}$ (relative to the hypothetical $\kappa = 0$ result) additional to that due to reduction, by molecular diffusion, of the maximum concentration. The latter effect is directly measured by the quantity α, with a reduction of the maximum from θ_1 to (order) αC_0. However, conservation of mass requires this reduction to be accompanied by an overall increase in the background concentration (from zero when $\kappa = 0$), and therefore a further reduction in the range of concentration values. Given that (3.5) describes the observations, it seems reasonable to interpret $\beta^{\frac{1}{2}}$ as the order of magnitude of this scale reduction.

However, since all moments are estimated from the same data record, there is an immediate inference that the quantities γ, δ, ..., introduced in (4.6) for the higher moments $\overline{c^3}, \overline{c^4}, \ldots$, satisfy (at least to an order of magnitude)

$$\beta^{\frac{1}{2}} = \gamma^{\frac{1}{3}} = \delta^{\frac{1}{4}} = \ldots. \tag{5.12}$$

Table 5 shows that, for the datasets considered in table 4 and figure 7, (5.12) is satisfied to a degree of accuracy that is remarkable given the semi-qualitative methods used to estimate γ and δ. A comparable degree of agreement for moments up to order 8, measured by Antonia & Sreenivasan (1976), can be inferred from results in table 1 of Chatwin & Sullivan (1987*b*). It might also be noted that the argument above suggests that values of β very near 1 arise only when there is relatively little reduction in the maximum concentration, i.e. when α is relatively high. This interpretation is consistent with the apparently anomalous results of Nakamura *et al.* (1987) discussed earlier where $\alpha = 3$ and $\beta = 1$; these experiments were in water (with a very low value of κ) unlike those of Gad-el-Hak & Morton (1979) that were in air (but otherwise the same).

The data analysis of this paper has been restricted to values of η over which β, as determined from figure 4, could be regarded as constant. Given the interpretation immediately above, it is interesting (and worth further investigation) that, for all the data examined, there is a wide range of such values of η. Nothing in this interpretation requires β to be constant and it is possible that (3.5), (4.6) and (5.12) could apply outside this range with β being a function of position.

5.3. *Instrument smoothing*

It has already been noted that increasing attention is being paid to the effects of instrument smoothing, i.e. to the differences between the measured and actual values of quantities like $\overline{c^2}, \overline{c^3}, \ldots$ caused by the inability of the measurement system adequately to resolve the fine-scale and high-frequency structure of the scalar field.

The reduction in the range of concentration values leading to (5.12) could be due in part to such smoothing, and – indeed – Chatwin & Sullivan (1987*a*) discussed whether the difference between β and 1 could be due entirely to this effect. The argument above, based on mass conservation, now shows this to be an untenable position; however, there is little doubt that part of the difference, perhaps a large part, could be due to instrument effects.

Important new experimental results by Sakai *et al.* (1989) on dye dispersion from a round jet in a water channel confirm the strong potential influence of instrument smoothing on β, and hence on perceived values of $\overline{c^2}, \overline{c^3}, \ldots$. Two different probes were used to measure the profiles of C and $\overline{c^2}$. In both cases the results satisfied the main hypothesis of this paper, viz. (3.5), and the two values of α were almost the same as that recorded by Becker *et al.* (1967) for a round jet of oil smoke in air; see table 2. However, the sampling volumes V_s of the two probes differed by a factor of about 70. The value of β for the larger probe ($V_s \approx 1.6 \times 10^{-10}$ m^3) was 0.160, again close to the value for the Becker *et al.* (1967) dataset. But the value of β for the smaller probe ($V_s \approx 2.4 \times 10^{-12}$ m^3) was 0.248, i.e. about 55% higher than for the larger probe. This corresponds to an increase of the same order in the perceived value of $\overline{c^2}$ at $\eta = 0$. Such results, and theoretical work such as that referred to elsewhere in this paper, suggest strongly that there is an urgent need for further experiments that specifically examine instrumentation effects on perceived concentration fluctuations. Without such experiments it will remain impossible to have full confidence in laboratory tests of theories.

5.4. *Concluding remarks*

The degree of agreement between the laboratory data discussed in this paper and the formula (3.5), the apparent robustness of some of the other proposed theoretical structure (e.g. its applicability, noted several times in the body of the paper, in other than self-similar conditions), and the algebraic simplicity of the formulae, make it plausible that the theory should be useful in predicting at least orders of magnitudes in many of the complicated practical problems to which concentration fluctuations are relevant. One important class is the assessment of hazards associated with the release of flammable or toxic gases following accidental loss of containment. In such cases, however, it is important to bear in mind the likely significant differences between actual and perceived fluctuations that were discussed immediately above.

It was noted at the beginning of this paper that its methodology is unusual, and does not relate to previous theoretical and computational approaches. It is intended to examine in the near future whether the simple algebraic models considered here are consistent with the equations governing quantities like C and $\overline{c^2}$, and how they relate to other approaches such as p.d.f. models, second-order closures, direct simulations and random walk calculations. In the field of containment dispersion research there is now a need for a thorough and critical comparison of the many techniques that are currently employed; it is hoped that the present contribution will be useful in this task.

We have been helped by many people, and we would particularly like to thank Professor R. A. Antonia, Dr Y. Sakai and Professor K. R. Sreenivasan, and our colleagues Dr Nils Mole (Brunel) and Dr Handson Yip (Western Ontario). We wish to acknowledge financial support from NATO (Research Grant No. RG.115.81), from the Natural Sciences and Engineering Research Council of Canada, and from the UK Ministry of Defence. Above all, it is appropriate to record how much we have learned

from George Batchelor, both in talking to him over the period of many years that began when we were students in his Department in the 1960s, and from reading his profound and original papers on turbulent diffusion.

REFERENCES

ANTONIA, R. A., BROWNE, L. W. B., CHAMBERS, A. J. & RAJAGOPALAN, S. 1983*a* Budget of the temperature variance in a turbulent plane jet. *Intl J. Heat Mass Transfer* **26**, 41–48.

ANTONIA, R. A., CHAMBERS, A. J. & ELENA, M. 1983*b* Points of symmetry in turbulent shear flows. *Intl Commun. Heat Mass Transfer* **10**, 395–402.

ANTONIA, R. A., PRABHU, A. & STEPHENSON, S. E. 1975 Conditionally sampled measurements in a heated turbulent jet. *J. Fluid Mech.* **72**, 455–480.

ANTONIA, R. A. & SREENIVASAN, K. R. 1976 Statistical properties of velocity and temperature fluctuations in a turbulent heated jet. *T.N. F.M.* 3. Dept of Mech. Eng., Univ. of Newcastle, NSW, Australia.

BATCHELOR, G. K. 1952 The effect of homogeneous turbulence on material lines and surfaces. *Proc. R. Soc. Lond.* A **213**, 349–366.

BATCHELOR, G. K. 1959 Small-scale variation of convected quantities like temperature in turbulent fluid. Part 1. General discussion and the case of small conductivity. *J. Fluid Mech.* **5**, 113–133.

BATCHELOR, G. K., HOWELLS, I. D. & TOWNSEND, A. A. 1959 Small-scale variation of convected quantities like temperature in turbulent fluid. Part 2. The case of large conductivity. *J. Fluid Mech.* **5**, 134–139.

BECKER, H. A., HOTTEL, H. C. & WILLIAMS, G. C. 1967 The nozzle-fluid concentration field of the round turbulent free jet. *J. Fluid Mech.* **30**, 285–303.

BIRCH, A. D., BROWN, D. R., DODSON, M. G. & THOMAS, J. R. 1978 The turbulent concentration field of a methane jet. *J. Fluid Mech.* **88**, 431–449.

BROWNE, L. W. B., ANTONIA, R. A. & CHAMBERS, A. J. 1984 The interaction region of a turbulent plane jet. *J. Fluid Mech.* **149**, 355–373.

CARN, K. K. & CHATWIN, P. C. 1985 Variability and heavy gas dispersion. *J. Haz. Mat.* **11**, 281–300.

CHATWIN, P. C. & SULLIVAN, P. J. 1979 The relative diffusion of a cloud of passive contaminant in incompressible turbulent flow. *J. Fluid Mech.* **91**, 337–355.

CHATWIN, P. C. & SULLIVAN, P. J. 1985 Effects of instrumentation and averaging on turbulent diffusion data. In *Proc. 5th Symp. on Turbulent Shear Flows, Cornell Univ., Ithaca, NY*, pp. 11.1–11.5.

CHATWIN, P. C. & SULLIVAN, P. J. 1987*a* Perceived statistical properties of scalars in turbulent shear flows. In *Proc. 6th Symp. on Turbulent Shear Flows, Toulouse, France*, pp. 9.1.1–9.1.6.

CHATWIN, P. C. & SULLIVAN, P. J. 1987*b* The probability density function for contaminant concentrations in some self-similar turbulent flows. In *Proc. 2nd Intl Symp. on Transport Phenomena in Turbulent Flows, Tokyo*, pp. 215–226.

CHATWIN, P. C. & SULLIVAN, P. J. 1989*a* The intermittency factor of scalars in turbulence. *Phys. Fluids* A **1**, 761–763.

CHATWIN, P. C. & SULLIVAN, P. J. 1989*b* The intermittency factor of dispersing scalars in turbulent shear flows. Some applications of a new definition. In *Proc. 7th Symp. on Turbulent Shear Flows, Stanford University*, pp. 29.4.1–29.4.6.

CHEVRAY, R. & TUTU, N. A. 1977 Conditional measurements in a heated turbulent jet. In *Structure and Mechanisms in Turbulence II* (ed. H. Fiedler), pp. 73–84. Springer.

DERKSEN, R. W. & SULLIVAN, P. J. 1987 Deriving contaminant concentration fluctuations from time averaged records. *Atmos. Environ.* **21**, 789–798.

DERKSEN, R. W. & SULLIVAN, P. J. 1989 Moment approximations for probability density functions. *Combust. Flame* (submitted).

DOWLING, D. R. & DIMOTAKIS, P. E. 1988 On mixing and structure of the concentration field of turbulent jets. In *Proc. AIAA/ASME/SIAM/APS 1st Natl Fluid Dyn. Cong., Cincinnati, Ohio. Part 2*, pp. 982–988.

DRAKE, M. C., SHYY, W. & PITZ, R. W. 1985 Superlayer contributions to conserved scalar pdfs in a H_2 turbulent jet diffusion flame. In *Proc. 5th Symp. on Turbulent Shear Flows, Cornell Univ., Ithaca, NY*, pp. 10.13–10.18.

EFFELSBERG, E. & PETERS, N. 1983 A composite model for the conserved scalar PDF. *Combust. Flame* **50**, 351–360.

FACKRELL, J. E. & ROBINS, A. G. 1982 Concentration fluctuations and fluxes in plumes from point sources in a turbulent boundary layer. *J. Fluid Mech.* **117**, 1–26.

GAD-EL-HAK, M. & MORTON, J. B. 1979 Experiments on the diffusion of smoke in isotropic turbulent flow. *AIAA J.* **17**, 558–562.

KENDALL, M. G. & STUART, A. 1977 *The Advanced Theory of Statistics, Vol. 1, Distribution Theory* (4th edn). London: Charles Griffin.

LARUE, J. C. & LIBBY, P. A. 1974 Temperature fluctuations in the plane turbulent wake. *Phys. Fluids* **17**, 1956–1967.

LARUE, J. C. & LIBBY, P. A. 1981 Thermal mixing layer downstream of half-heated turbulence grid. *Phys. Fluids* **24**, 597–603.

MOLE, N. 1989 Estimating statistics of concentration fluctuations from measurements. In *Proc. 7th Symp. on Turbulent Shear Flows, Stanford University*, pp. 29.5.1–29.5.6.

MOLE, N. 1990 A model of instrument smoothing and thresholding in measurements of turbulent dispersion. *Atmos. Environ.* (to appear).

MOLE, N. & CHATWIN, P. C. 1987 Assessing and modelling variability in dispersing vapour clouds. In *Proc. Intl Conf. on Vapor Cloud Modeling, Cambridge, Mass* (ed. J. L. Woodward), pp. 779–800. AIChE.

NAKAMURA, I., SAKAI, Y. & MIYATA, M. 1987 Diffusion of matter by a non-buoyant plume in grid-generated turbulence. *J. Fluid Mech.* **178**, 379–403.

PITTS, W. M. & KASHIWAGI, T. 1984 The application of laser-induced Rayleigh light scattering to the study of turbulent mixing. *J. Fluid Mech.* **141**, 391–429.

SAKAI, Y., NAKAMURA, I., TSUNODA, H. & SHENGIAN, L. 1989 On the influence of disturbances generated by obstacles on point source plume diffusion in grid turbulence. Characteristics of concentration fluctuations and conditional statistics. Manuscript in preparation. (Material presented at *Euromech 253, Brunel University, 30 August–1 September 1989*).

SHAUGHNESSY, E. J. & MORTON, J. B. 1977 Laser light-scattering measurements of particle concentration in a turbulent jet. *J. Fluid Mech.* **80**, 129–148.

SREENIVASAN, K. R. 1981 Evolution of the centerline probability density function of temperature in a plane turbulent wake. *Phys. Fluids* **24**, 1232–1234.

SREENIVASAN, K. R., DANH, H. Q. & ANTONIA, R. A. 1976 Diffusion from a heated wall-cylinder immersed in a turbulent boundary layer. In *Proc. Thermofluids Conf., Hobart, Inst. of Engineers, Australia*, pp. 103–106.

SULLIVAN, P. J. 1984 Whence the fluctuations in measured values of mean-square fluctuations? In *Proc. 4th Joint Conf. on Applications of Air Pollution Meteorology, Portland, Oregon* (ed. G. A. Beals and N. E. Browne), pp. 115–121. American Meteorological Society, Boston.

WILSON, D. J., ROBINS, A. G. & FACKRELL, J. E. 1982 Predicting the spatial distribution of concentration fluctuations from a ground level source. *Atmos. Environ.* **16**, 497–504.